LA-UR-87-3444

TITLE DYNAMICAL CORRELATIONS FROM MOBILE VORTICES IN TWO-DIMENSIONAL EASY-PLANE FERROMAGNETS

AUTHOR(S): F. G. Mertens
A. R. Bishop
G. M. Wysin
C. Kawabata

SUBMITTED TO: Physical Review B 39 591 (1989)

DYNAMICAL CORRELATIONS FROM MOBILE VORTICES IN TWO-DIMENSIONAL EASY-PLANE FERROMAGNETS

F. G. Mertens[†], A. R. Bishop, G. M. Wysin
Theoretical Division and Center for Nonlinear Studies
Los Alamos National Laboratory
Los Alamos, NM 87545, USA
and
C. Kawabata
Okayama University Computer Center
Okayama, 700, Japan

Abstract

Assuming an ideal gas of unbound vortices above the Kosterlitz-Thouless transition temperature, the dynamic form factors are calculated for both the in-plane and out-of-plane correlations. In both cases central peaks are predicted which are, however, produced by quite different mechanisms, depending on whether the correlations are globally or locally sensitive to the presence of the vortices. For the in-plane correlations the wavevector dependencies of the width and intensity of the peaks are very well supported by the central peaks, which are observed in a combined Monte Carlo-molecular dynamics simulation of the XY-model. Therefore, the parameters of the theory (rms vortex velocity and mean vortex-vortex separation) can be fitted and turn out to agree rather well with independent theoretical estimates. Recent inelastic neutron scattering experiments on the in-plane correlations for $BaCo_2(AsO_4)_2$ and Rb_2CrCl_4 also show central peaks. Their temperature and wavevector dependencies are consistent with our results, but their widths are larger than the theoretical estimates. Therefore, these peaks are interpreted to result, as least partially, from a gas of vortices. For the out-of-plane correlations our simulations also show a central peak. However, so far it cannot be identified unequivocally as a vortex contribution.

[†] Permanent address: Physics Institute, University of Bayreuth, D-8580 Bayreuth, Fed. Rep. of Germany

1. Introduction

The increasing emergence of examples of well-characterized quasi-two-dimensional (2-D) magnetic materials has been prompted by technical advances in artificially structured, layered and surface-layer materials. More recently there has also been renewed attention to accurate inelastic neutron scattering measurements at low frequencies and long wavelengths in quasi 2-D magnets. It is therefore an appropriate time for detailed studies of 2-D spin dynamics. One particularly interesting case concerns materials with easy-plane symmetry, where we can probe dynamics associated with strongly nonlinear collective structures such as vortices and domains. For example, in pure easy-plane symmetry we expect that a Kosterlitz-Thouless[1] (K-T) type of topological phase transition will occur, with vortex-antivortex pairs beginning to unbind above a critical temperature T_c. In this regime it is then natural to ask whether there are dynamical signatures of the low density of unbound vortices. This is the principal concern of the present work.

Candidate materials are increasing rapidly and include: K_2CuF_4, Rb_2CrCl_4, $BaM_2(XO_4)_2$ (M = Co, Ni, ...; X = As, P, ...) and other layered magnets;[2-5] magnetically-intercalated graphites, e.g. $CoCl_2$-GIC prepared with various stagings;[6] and magnetic surface layers (e.g. magnetic lipids or magnetic epitaxial layers).[7] Treated within localized (Heisenberg) spin models (below), the ratio of inter- to intra-plane magnetic coupling constant is typically 10^{-3} - 10^{-6}. Furthermore, a great variety of magnetic interactions can be tuned by varying the material -- from ferromagnetic, to antiferromagnetic (e.g. $BaNi_2(PO_4)_2$), to competing nearest and next-nearest neighbors (e.g. $BaCo_2(AsO_4)_2$. These can have various degrees of (crystal field) symmetry-breaking in

the easy plane, leading to domain patterns which compete with the characteristic vortex structures of the easy-plane symmetry.

Clearly this field is very rich in terms of materials and raises some fundamental questions with regard to nonlinear spin dynamics -- in much the same way that quasi-1-D magnets have challenged theoretical frameworks in the last decade.[8,9] Although dynamics associated with K-T theory has been studied successfully in the topologically equivalent problems of 2-D superfluids,[10] superconducting granular films,[11] and 2-D Josephson junction arrays,[12] comparable studies have not been made for 2-D magnets, except for some renormalized spin-wave approaches[13,14] and partial vortex-spinwave "phenomenologies" (below).

Since the scenario of vortex-antivortex pair unbinding introduced by K-T has been so successful for thermodynamic properties, it is important to test its predictive power for dynamics. Therefore, we will focus here on the phenomenology of an ideal, dilute gas of free vortices above T_c moving in the presence of renormalized spin waves and screened by the remaining vortex-antivortex bound pairs. Such an approach, explicitly incorporating the nonlinear coherent excitations, is similar in spirit to "soliton-gas" approaches for 1-D magnets[8] and has already been advocated by Huber.[15] However, he calculated only vortex autocorrelation functions, leading to dynamic form factors without any wavevector dependence. Here we will calculate full form factors $S(\vec{q},\omega)$, and compare them with recent simulations[16] (Monte Carlo-molecular dynamics (MC-MD)) as well as inelastic neutron scattering data[17,18,5] -- both simulations and experiments have found anomalous "central peak" structures (i.e. scattering intensity near $\omega = 0$) for $T > T_c$, and indeed scattering from a vortex gas will be identified here as one mechanism for such a central peak.

In this paper we consider only the simplest situation of pure easy-plane spin symmetry. (Results for more general cases will be presented elsewhere.) However, dynamics necessarily involves some out-of-plane spin motion. Therefore, we treat explicitly the anisotropic Heisenberg model with classical Hamiltonian

$$H = - J \sum_{(m,n)} [S_x^m S_x^n + S_y^m S_y^n + \lambda S_z^m S_z^n] \quad , \tag{1.1}$$

where (m,n) label near-neighbor sites on a 2-D square lattice, J is a ferromagnetic coupling constant, and the classical spin vector is $\vec{S}^m = (S_x^m, S_y^m, S_z^m)$. The XY and isotropic Heisenberg limits correspond to $\lambda = 0$ and 1, respectively. Note that $\lambda = 0$ does not correspond to the "planar" limit[1] where spins are strictly confined to the XY plane. However, critical properties for the in-plane spin components (S_x or S_y) are still those of K-T theory -- e.g. with static spin-spin correlations changing from exponential to power law as T is decreased below T_c. By contrast the static correlations for the out-of-plane component (S_z) are exponential both above and below T_c (possibly with higher order signatures at T_c and the specific heat maximum at $T_s > T_c$).[19] The variation of T_c with λ is experimentally important. Both vortex theory[21] and MC results[20] show that T_c is only weakly-dependent on λ except for λ very close to 1, when $T_c \to 0$. Thus, even materials with very weak easy-plane anisotropy (e.g., $\lambda \simeq 0.99$ in K_2CuF_4) have a substantial K-T transition temperature and 2-D fluctuation regime -- the true ordering, sufficiently close to the actual transition, is of course 3-D in real materials. For the materials mentioned above, coupling constants have been estimated from fits to, e.g. linear spin wave theory, and λ values are in the range 0.4 - 0.99, where $T_c^{2\text{-}D}$ is still close to $T_c^{2\text{-}D}(\lambda = 0)$.

We will need to make use later of thermodynamic results of K-T theory. Assuming we can adopt planar limit results as a guide, the relevant information for our purposes primarily concerns the static correlations[22-25]

$$S_{xx}(r) \sim r^{-1/2} \exp(-r/\xi(T)) \quad , \quad T > T_c \tag{1.2}$$

where ξ is the correlation length and

$$\xi(T) = \xi_0 \exp(b\tau^{-1/2}) \quad , \quad \tau \equiv (T-T_c)/T_c \quad . \tag{1.3}$$

ξ_0 is on the order of the lattice constant, and b has been found[25] to be quite temperature-dependent even for small τ. The correlation length can be further interpreted[10] as half of the mean separation between free vortices:

$$n_v(\tau) \simeq (2\xi)^{-2} \quad , \tag{1.4}$$

with n_v the free vortex density. Of course, these should only be viewed as order-of-magnitude relations, since the vortex creation energy itself decreases as λ increases'[21] and full thermodynamics of the anisotropic Heisenberg model (1.1) are not available. Although such effects can be partially included, we prefer to leave form (1.3) and compare it with fits of ξ to our numerical data (below). Ultimately a direct estimate of n_v from numerical simulations (following individual vortex dynamics) may itself be possible, cf. ref. 26.

As in 1-D easy-plane magnets, careful distinction must be made between <u>in-plane</u> and <u>out-of-plane</u> dynamic correlations. In addition to the remarks concerning critical properties above, we will find in section 2 that a central peak for $S_{xx}(\vec{q},\omega)$ is predicted to arise above T_c

from a vortex gas. The correlations reveal the mean vortex-vortex separation 2ξ and the rms vortex velocity $\bar{u}$. These phenomenological parameters are determined by fitting the width and intensity of the predicted central peak to the corresponding quantities from our MC-MD simulations. The results are compared with theoretical estimates: ξ from (1.3) and $\bar{u}$ from the velocity autocorrelation function of Huber.[15] (In our publication[40] of preliminary results we did not fit the parameters but rather used the theoretical estimates.)

Besides the central peaks, our MC-MD results also show spin-wave contributions. Above T_c these are strongly softened for S_{xx} (consistent with the "universal jump" prediction[27]), but not for S_{zz}. Moreover, there seem to be multi-magnon contributions, especially for S_{zz}.

In section 3 our results are compared with recent inelastic neutron scattering experiments. So far central peaks in $S_{xx}(\vec{q},\omega)$ have been reported for Rb_2CrCl_4 (ref. 17) and $BaCo_2(AsO_4)_2$ (refs. 18, 5). We discuss in detail the ω-, q-, and temperature dependencies of the peaks.

In section 4, $S_{zz}(\vec{q},\omega)$ is calculated assuming that the out-of-plane structure of moving vortices can be approximated by the static structure. The width of the predicted central peak is consistent with our MC-MD results, but not the intensity. We conclude that the velocity dependence of the out-of-plane structure must be incorporated.

Section 5 contains a summary and a discussion of the limitations of the present theory, and of possible modifications which take into account the great variety of different interactions and symmetries of the real materials.

2. In-Plane Correlations

We use a continuum description and spherical coordinates for a general time-dependent spin configuration:

$$S_x(\vec{r},t) = S\cos\phi(\vec{r},t)\sin\theta(\vec{r},t)$$

$$S_z(\vec{r},t) = S\cos\theta(\vec{r},t) \qquad (2.1)$$

with $\vec{r} = (x,y)$. Consider a single vortex at the origin:

$$\phi(\vec{r}) = \pm \tan^{-1}(y/x) \quad . \qquad (2.2)$$

The form of $\theta(\vec{r})$ will be discussed in section 4. The vortex solutions have the asymptotic properties

$$\theta_{\pm}(r) = \begin{cases} \frac{\pi}{2}\left[1 \mp \exp(-r/r_v)\right] & , r \gg r_v \qquad (2.3a) \\ 0 \text{ or } \pi & , r \to 0 \qquad (2.3b) \end{cases}$$

with vortex-core "radius" r_v. S_z is localized and correlations are sensitive to the vortex size and shape (section 4). By contrast, S_x (and S_y) are not localized, i.e. they have no spatial Fourier transform. Therefore the in-plane correlation function $S_{xx}(\vec{r},t) = \langle S_x(\vec{r},t)\, S_x(\vec{0},0)\rangle$ is only globally sensitive to the presence of vortices, which act to break long-range order in $\cos\phi$. Thus the characteristic length is the mean vortex-vortex separation 2ξ.

Consider first the field $\cos\phi(\vec{r},t)$ in $S_x = S\cos\phi\sin\theta$. As seen in Fig. 1 for a particular case, every vortex that passes with its center between $\vec{0}$ and $\vec{r}$ in time t diminishes the correlations, changing $\cos\phi$ by a factor of (-1), independent of the direction of movement. In

this sense vortices act like "2-D sign functions." Inclusion of the field $\sin\theta(\vec{r},t)$ in S_x, with θ given by (2.3), shows that the change of sign does not occur abruptly, but over the distance $2r_v$. This means that vortices behave effectively as "2-D kinks" with half width r_v. Considering length scales $>> r_v$ the dominant effect of the moving vortices are the above-mentioned changes of sign. Thus an ideal vortex gas gives

$$S_{xx}(\vec{r},t) = S^2 \langle\cos^2\phi\rangle\langle(-1)^{N(\vec{r},t)}\rangle \quad . \tag{2.4}$$

Here $N(\vec{r},t)$ is the number of vortices which pass an arbitrary, non-intersecting contour connecting $(\vec{0},0)$ and $(\vec{r},t)$; the average over $\cos^2\phi$ is 1/2, assuming a random spin configuration outside of the vortex cores.

Expressions like (2.4) were evaluated by several authors for the case of kinks in 1-D models (e.g. ϕ^4 or sine-Gordon), see ref. 8 and references cited therein. A very detailed investigation was made by Dorogovtsev,[29] who also calculated such correlations numerically in two dimensions. We have adopted his general procedure and, by implementing several modifications, we identify certain cancellations which allow us to calculate (2.4) analytically. We will demonstrate this for the 1-D case, the generalization to higher dimensions will then be straightforward.

For simplicity all kinks are first taken to have the same velocity u. Considering the case $x \geq ut > 0$, we choose the velocity-independent

contour $(0,0) \to (x,0) \to (x,t)$, which is outside of the "light" cone $x = \pm ut$. The contribution from the first part of this contour is

$$\langle(-1)^{N(x,t)}\rangle = \sum_{n_\ell} (-1)^{n_\ell} p(n_\ell) \sum_{n_r} (-1)^{n_r} p(n_r) \quad . \tag{2.5}$$

Because we assumed a dilute ideal gas, we have a Poisson distribution, $p(n_\ell) = \bar{n}_\ell^{\,n_\ell}/n_\ell!\, \exp(-\bar{n}_\ell)$, where n_ℓ and n_r are the numbers of kinks in $[0,x]$ running to left and to right, respectively; $\bar{n}_\ell$ and $\bar{n}_r$ are the average numbers. Kinks pass this part of the contour at the same time $(t=0)$ but at different positions, implying that these events are not correlated. Thus n_ℓ and n_r are independent, and the two sums in (2.5) can be calculated separately, giving $\exp(-2\bar{n}_\ell - 2\bar{n}_r) = \exp(-x/\xi)$, for (2.5). For the second part of the contour, $(x,0) \to (x,t)$, we obtain formally the same expression as (2.5), but with n_ℓ the number of left-running kinks in $[x, x + ut]$, and n_r the number of right-running kinks in $[x - ut, x]$. Kinks pass the same point at different times. Events are correlated as long as $t < x/u$, which is just the case we are considering. Thus n_ℓ and n_r are not independent. Assuming $n_\ell = n_r$, then $(n_\ell + n_r)$ is even, implying that there is no contribution from the second part of the contour.

Now consider the second case, $ut \geq x > 0$. We choose the contour $(0,0) \to (0,t) \to (x,t)$, inside the light cone. The same type of argument shows that the vertical component $(0,0) \to (0,t)$ gives a contribution, whereas the horizontal part $(0,t) \to (x,t)$ does not -- precisely opposite to the first case. The result for (2.5) is $\exp(-ut/\xi)$, in contrast to $\exp(-x/\xi)$ in the first case. Both cases can be combined into the final result,

$$\langle(-1)^{N(x,t)}\rangle = \exp\left\{-\frac{|x-ut|}{2\xi} - \frac{|x+ut|}{2\xi}\right\} \quad . \tag{2.6a}$$

The 2-D calculation, where the vortices play the role of the kinks, proceeds in a similar way (Appendix B). Including an average over all velocities $u = |\vec{u}|$, we have

$$\langle(-1)^{N(\vec{r},t)}\rangle = \exp\left\{-\int_0^\infty \left[\frac{|r-ut|}{2\xi} + \frac{|r+ut|}{2\xi}\right] \tilde{P}(u)\, du\right\} \quad . \tag{2.6b}$$

In order to obtain the velocity distribution we consider the velocity $\vec{u}$ of a vortex at $\vec{R}$ which results from an equation of motion.[15] $\vec{u}$ is proportional to $\hat{z} \times \vec{F}$; here $\hat{z}$ is a unit vector perpendicular to the XY-plane and $\vec{F}$ is the net force due to the interactions with the other vortices at $\vec{R}_\nu$. These forces are proportional to $\vec{R} - \vec{R}_\nu$ and decrease with increasing distance. A perfectly symmetric array of the $\vec{R}_\nu$ would yield a zero net force and thus zero velocity. However, the density of vortices is homogeneous only on the average, locally the distribution is random. Therefore, the deviations from the average $\vec{u} = 0$ follow a Gaussian normal distribution, i.e. we can assume a Maxwellian velocity distribution $P(\vec{u})$. For the distribution $\tilde{P}(u)$ of the moduli we get $\tilde{P}(u) \sim u$ times a Gaussian (Appendix B). The integration over u in (2.6b) eventually leads to

$$S_{xx}(\vec{r},t) = \frac{1}{2} S^2 \exp\left\{-\frac{r}{\xi} - \frac{\sqrt{\pi}}{2}\frac{\bar{u}|t|}{\xi} \operatorname{erfc}\left(\frac{r}{ut}\right)\right\} \quad , \tag{2.7}$$

where $\bar{u}$ is the root-mean-square velocity and erfc is the complementary error function. Similarly to the 1-D case[30], there is an excellent

analytic approximation for (2.7), which preserves not only the integrated intensity (see below) but also the correct asymptotic behavior for r or t → ∞. Namely,

$$S_{xx}(\vec{r},t) \simeq \frac{1}{2} S^2 \exp\{-[(r/\xi)^2 + (\gamma t)^2]^{\frac{1}{2}}\} \quad , \tag{2.8}$$

with $\gamma = \sqrt{\pi}\ \bar{u}/(2\xi)$. Using approximation (2.8), both the spatial and temporal Fourier transforms can be performed, yielding (Appendix C)

$$S_{xx}(\vec{q},\omega) = \frac{S^2}{2\pi^2} \frac{\gamma^3 \xi^2}{\{\omega^2 + \gamma^2[1 + (\xi q)^2]\}^2} \quad . \tag{2.9}$$

This is a (squared) Lorentzian central peak (c.p.) with q-dependent width

$$\Gamma_x(q) = \frac{1}{2} [\pi(\sqrt{2} - 1)]^{\frac{1}{2}} \frac{\bar{u}}{\xi} \sqrt{1 + (\xi q)^2} \quad , \tag{2.10}$$

and integrated intensity

$$I_x(q) = \frac{S^2}{4\pi} \frac{\xi^2}{[1 + (\xi q)^2]^{3/2}} \quad . \tag{2.11}$$

(Result (2.11) can be checked by performing the Fourier transform of (2.7) with t = 0).

Note that $I_x \sim \xi^2 \sim n_v^{-1}$, as expected since the correlations are diminished by the presence of the vortices. (In contrast to the out-of-plane correlations where $I_z \sim n_v$, see section 4).

We now compare the predictions of this phenomenological theory with the results of our MC-MD simulation. For these simulations we have used Hamiltonian (Landau) spin dynamics $d\vec{S}_n/dt = \{\vec{S}_n, H\}$ with Hamiltonian

(1.1) on an isotropic square lattice with a size up to 100 × 100, giving accurate access to wave numbers $\gtrsim 0.02\ \pi/a$. The MC-algorithm[19] used 10^4 MCS per spin to equilibrate 3 random initial configurations. Then MD with 4th-order Runge-Kutta was applied, with timestep 0.04, sampling time NS × 0.04, NS = 4, 8, 32, and total integration time 512 × NS × 0.04. This is in units where $J = k_B = a = S = 1$. Further details are given in Appendix D.

Figure 2 shows $S_{xx}(\vec{q},\omega)$ from our MC-MD simulations for the XY-model. The spin waves are strongly softened for $T > T_c$, consistent with the theoretical predictions[27] of a "universal jump" as well as with experiments.[2,17,18,5] However, the spin-wave softening depends[14] on q, i.e. on the length scale over which vortices are considered to be free (c.f. the analogous situation in 2-D superfluids[10] and 2-D Josephson junction arrays[12]). Therefore we observe for small q only a central peak; for large q broad spin-wave contributions can be distinguished besides the c.p.

The predicted q-dependence (2.10) of the c.p. width is very well supported by the MD data (Fig. 3). For $q \gg \xi^{-1}$, we have $\Gamma_x = 0.57\ \bar{u}q$, and a fit of $\bar{u}$ gives the numbers in Table 1; they can be compared with a formula of Huber[15] obtained from the velocity autocorrelation function using an equation of motion for free vortices:

$$\bar{u}^2 = \frac{\pi}{2}\left(\frac{JS^2a^2}{\hbar}\right)^2 n_v \ln\left(\frac{k_B T_c}{JS^2 n_v a^2}\right) . \qquad (2.12)$$

The logarithmic term can be approximated using (1.3), (1.4), and $\xi_0 = a$. With $T_c \simeq 0.8$ (ref. 19) we get

$$\bar{u} = \frac{\sqrt{\pi}}{2} \exp(-b/\sqrt{\tau}) \; (b/\sqrt{\tau} + 0.58)^{1/2} \quad . \tag{2.13}$$

This formula predicts a strong increase of $\bar{u}$ for small τ and a nearly constant behavior above about $\tau = 4b^2 = 0.36$, with $b \tilde{\sim} 0.3$ for this τ (see Ref. 25). This increase and the saturation both agree qualitatively with the simulations,[16] but the absolute values for $\bar{u}$ are about a factor of 2 smaller than observed (Table 1). Note however, that b(T) is not well known for the lower temperatures in Table 1, and for ξ_0 only the order of magnitude is known.

For $q \ll \xi^{-1}$, (2.10) reduces to $\Gamma_x = 0.57 \; \bar{u}/\xi$. Using (1.3) and (2.13), the constant regime begins here at a much higher temperature, $\tau \simeq 16b^2$, which is outside of the regime of our simulations. Since $\bar{u}$ is already known, ξ can now also be fitted; the agreement with the KT-formula (1.3) is rather good (Table 1).

The correlation length can also be obtained by fitting (2.11) to the c.p. intensity. Assuming a squared Lorentzian form, we estimate the intensity by $I_x = \pi(4(\sqrt{2}-1))^{-\frac{1}{2}} \Gamma_x \cdot S_{xx}(q,0)$. This can be compared with the total intensity $I_x^{tot} = S_{xx}(q,t=0)$ and shows that I_x^{tot}, for $q \ll \xi^{-1}$, essentially consists of a central peak with the q-dependence of (2.11). This is consistent with theory: the Fourier transform of (1.2) gives

$$I_x^{tot}(q) \sim 1 - \frac{15}{16} (\xi q)^2 \quad , \quad \text{for } q \ll \xi^{-1} \quad ; \tag{2.14}$$

this q-dependence is the same as that of the vortex contribution (2.11) (apart from a constant factor). The spin-wave contributions (Appendix E) have quite a different q-dependence, namely $q^{-(2-\eta)}$ (except for $q < O(L^{-1})$, where L is the lattice size); the critical exponent[22] η is

1/4 for $T \gtrsim T_c$. The spin waves are important only for larger q -- for $q \gg \xi^{-1}$ they exceed the vortex contributions which decrease like q^{-3}.

Figure 4 shows that the predicted q-dependence (2.11) of I_x is indeed observed for small q, which is consistent with our theory working on a length scale $>> r_v$. The fits for ξ turn out to be close to those obtained above (Table 1).

The absolute value of the intensity that we observe in the MC-MD simulations is about a factor of 5 smaller than expected from (2.11). This might be due to our neglect of effects from the finite size of the vortices, e.g. the sinθ correlations have been omitted in (2.4).

For $T \gg T_c$ we expect a simple diffusive central peak for the hydrodynamic regime,[15] i.e. for $q \lesssim n_v^{1/2} = (2\xi)^{-1}$. Then the density of free vortices is too high for our dilute gas approach.

Finally, we comment on Huber's results[32,15] for the in-plane correlations. He also finds that the motion of free vortices diminishes the correlations, but concludes that there is no qualitative effect on the autocorrelation functions (in contrast to the out-of-plane case). However, our MC-MD data clearly show a distinct central peak. One reason for this discrepancy may be that Huber assumed that $\phi(\vec{r},t) - \phi(\vec{r},0)$ is small; this fails when a vortex passes the point $\vec{r}$.

3. Comparison with Experiments

So far our theory has been tested by MC-MD simulations only for the XY-limit, $\lambda = 0$. However, central peaks have been seen in real quasi-2-D magnetic materials with finite λ, e.g. $\lambda \simeq 0.4$ for $BaCo_2(AsO_4)_2$ and $\lambda = 0.99$ for K_2CuF_4. In this respect, it is important

to note again that the transition temperature T_c decreases very little with increasing λ for a wide λ range;[19-21] only when λ is very close to 1 does T_c change considerably, and eventually goes to zero for $\lambda \to 1$ -- neglecting 3-D ordering. Other properties can depend much more on λ. For example, the spin-wave frequencies from Hamiltonian (1.1) are (with $a = 1$)

$$\omega^2 = (4JS)^2[(1 - \tfrac{1}{2}(\cos q_x + \cos q_y)][1 - \tfrac{\lambda}{2}(\cos q_x + \cos q_y)]. \quad (3.1)$$

For $q = (q_x^2 + q_y^2)^{\frac{1}{2}} \ll \pi$ and $1-\lambda \ll 1$, we get

$$\omega^2 = (2JS)^2[(1-\lambda)\, q^2 + \tfrac{1}{4} q^4] \quad , \quad (3.2)$$

and we expect a crossover from the linear dispersion of the XY model to the quadratic dispersion of the isotropic Heisenberg model at $q^* \simeq 2(1-\lambda)^{1/2}$. (This definition differs by a factor of $\sqrt{2}$ from that of ref. 2). We have made simulations for $\lambda = 0.8$ which indeed show this crossover at about $q^* = 0.285\ \pi/a$ -- see Figure 5.

The vortex-core radius r_v in (2.3) also depends strongly on λ, see section 4. Because we have been working on a length scale large compared to r_v, we expect our phenomenological vortex-gas theory to hold only for

$$q \ll r_v^{-1} = a^{-1}\, 2\sqrt{(1-\lambda)/\lambda} \quad . \quad (433)$$

Fig. 6 shows the width of the central peak for $\lambda = 0.8$ at $T = \bar{0}.9$. The predicted q-dependency (2.10) is seen in fact for $q \ll r_v^{-1} = 0.32\ \pi/a$. For larger q the behavior is qualitatively similar to that observed in our simulations for the isotropic Heisenberg model and will have to be

explained by another theory, presumably including instanton excitations.[33,34]

A fit of Γ_x for $q \ll 0.32\pi/a$ gives $\bar{u} = 0.45$ and $\xi = 6.4a$. The smaller value for $\bar{u}$, compared to the XY limit, can be understood qualitatively: the interactions[21] which themselves induce the motion of the free vortices become smaller with increasing λ and eventually go to zero for $\lambda \to 1$.

Fortunately, the inelastic neutron scattering experiments that have revealed central peaks have been made so far for very small q and intermediate λ-values. This means that our theory should hold in these cases. Presently, the published experimental results are rather incomplete. In particular, the out-of-plane correlations have not yet been measured at all.

For $BaCo_2(AsO_4)_2$ a Lorentzian central peak has been fitted.[18,5] The width is about 0.3 MeV at T = 6K for $q = 0.02\pi/a$. The theoretical width from (2.10) is $\Gamma_x = 0.57\ \bar{u}/\xi$, for $q \ll \xi^{-1}$. For $\bar{u}$ we can take Huber's formula (2.12) directly because the correlation length ξ (and thus n_v) is known from quasi-elastic neutron scattering.[4,5] In this way we avoid using (1.3), where ξ_0 and b are not well known. From ref. 5 we take $T_c = 5.4 \pm 0.2$K, an effective nearest-neighbor coupling constant $J = 30 \pm 3$K, and $\xi = 16\mathring{A} = 3.2a$ (for T = 6K) and obtain $\Gamma_x \simeq 0.04$ MeV.

Several important points have been neglected in the above comparison: the Co^{++} ions form a honeycomb lattice, whereas a square lattice was assumed in Huber's formula; the correlation length has been estimated from $\xi = (\xi_{\parallel} \cdot \xi_{\perp})^{\frac{1}{2}}$ with $\xi_{\parallel} = 9\mathring{A}$ and $\xi_{\perp} = 30\mathring{A}$ (for T = 6K). This strong in-plane anisotropy has not yet been included in our theory. Surprisingly, the estimate $\xi = 3.2a$ corresponds to $b = 0.4$ (for $\xi_0 = a$),

which fits well to the values of b used in Table 1 for this temperature range. Last but not least, the spins S = ½ for the Co^{++} ions certainly should be treated quantum mechanically (see below).

In addition to the absolute values for Γ_x we can also compare with its reported temperature dependence. Below T_c there is already a central peak with a resolution-limited width of about 0.08 meV. Above T_c there is a very strong increase of Γ_x with temperature, and no saturation is observed (for $T \leq 6.5K$). This behavior is qualitatively similar to that of $\Gamma_x = 0.57\ \bar{u}/\xi$ with $\bar{u}$ from (2.13) -- see the discussion in section 2. Our interpretation is that the observed central peak comprises two parts: a weakly temperature-dependent contribution plus a contribution from the unbound vortices above T_c. The former contribution may result from ordered domains that are favored by the in-plane symmetry-breaking fields;[35] a constant contribution would come from, e.g. isotope or impurity effects.

In Rb_2CrCl_4 the $Cr^{++}(3d)^4$ ions have spin S = 2 and lie in planar square arrays. The coupling constant J is 14.4K = 1.24 meV. T_c = 45.5K has been obtained from measurements of the susceptibility.[36] With inelastic neutron scattering, a central peak has been measured which was fitted to a product of two Lorentzians, one for the ω-dependence and one for the q-dependence.[17] The width is about 0.05 meV for q = 0.014 $\mathring{A}^{-1}$ at T = 51.08K. Unfortunately, different values for ξ have been obtained by different methods. The above mentioned fit yields a constant ξ = 137 $\mathring{A}$ = 27a for temperatures below the 3-D ordering temperature T_c^{3D} = 52.2K. Thus this correlation might be a 3-D effect; above 52.2K, ξ decreases with increasing temperature. On the other hand, a fit of the susceptibility to $\chi \sim \xi^{2-\eta}$ with ξ from (1.3) yields an anomalously high

value b = 2.3; this would give ξ = 750a for T = 51K. However, this fit was made in the temperature range $0.7 < \tau < 1.3$, where the KT-formula (1.3) probably no longer applies. Therefore, at the moment we can identify only an upper bound for Γ_x, considering ξ = 27a to be a lower bound. We obtain $\Gamma_x(q = 0) = 0.57\ \bar{u}/\xi < 0.007$ meV. We still have to consider here the $(1+(\xi q)^2)^{1/2}$ factor in (2.10) because of the large ξ; this eventually gives $\Gamma_x < 0.02$ meV for $q = 0.014\ \mathring{A}^{-1}$.

In contrast to $BaCo_2(AsO_4)_2$, there are also some reported features about the q-dependence of Γ_x, which can be compared with the prediction (2.10). For $T < T_c^{3D}$, the width increases approximately linearly with q; because of the large ξ probably only the linear part of (2.10) (for $\xi q >> 1$) is seen here (c.f. Fig. 3a). At T_c the width is finite, increasing quadratically with q for $T > T_c^{3D}$. There ξ drops, therefore the small-q behavior of (2.10), namely a constant plus a quadratic term, might be seen. A more accurate comparison will be possible when data on the q-dependence is available.

4. Out-of-Plane Correlations

In contrast to S_{xx} the out-of-plane correlation function $S_{zz}(\vec{r},t)$ is locally sensitive to the presence of vortices because S_z is localized for a single vortex (see below).

We assume that an arbitrary configuration of the field $\theta(\vec{r},t)$ in $S_z = S\cos\theta$ can be represented by a sum of spin-wave and vortex contributions. Above T_c, the latter contribution is taken to be produced by a dilute gas of N_v unbound vortices with positions $\vec{R}_v$ and velocities $\vec{u}_v$

$$\theta(\vec{r},t) = \sum_{\nu=1}^{N_v} \theta(\vec{r} - \vec{R}_\nu - \vec{u}_\nu t) \quad . \tag{4.1}$$

Considering only incoherent scattering from independent vortices the same superposition also holds for S_z

$$S_z(\vec{r},t) \simeq S \sum_{\nu=1}^{N_v} \cos\theta(\vec{r} - \vec{R}_\nu - \vec{u}_\nu t) \quad . \tag{4.2}$$

Thermal averaging is incorporated by averaging with respect to the vortex positions and velocities. In this way it is easily seen that $\langle S_z(\vec{r},t)\rangle = 0$, assuming that there is the same number of the two types of vortices (±) in (2.3).

In the same way, $S_{zz}(\vec{r},t) = \langle S_z(\vec{r},t)S_z(\vec{0},0)\rangle$ is calculated as

$$S_{zz}(\vec{r},t) = n_v S^2 \iint d^2R\, d^2u\, P(\vec{u}) \cos\theta(\vec{r} - \vec{R} - \vec{u}t) \cos\theta(\vec{R}) \quad , \tag{4.3}$$

where n_v is the density of free vortices, and $P(\vec{u})$ is the single vortex velocity distribution.

In our publication of preliminary results[40] we have assumed that the out-of-plane structure of a moving vortex can be approximated by the static structure. This would mean that the function $\theta(\vec{r})$ in the vortex form factor

$$f(\vec{q}) = \int d^2r \cos\theta(\vec{r}) e^{-i\vec{q}\vec{r}} \tag{4.4}$$

does not depend on the velocity and is isotropic. In this case the spatial Fourier transformation of (4.3) yields

$$S_{zz}(\vec{q},t) = \left(\frac{S}{2\pi}\right)^2 n_v |f(q)|^2 \int d^2u\, P(\vec{u}) e^{-i\vec{q}\vec{u}t} \quad . \tag{4.5}$$

Using again a Maxwellian $P(\vec{u})$, the temporal Fourier transformation gives a dynamic form factor exhibiting a Gaussian central peak

$$S_{zz}(\vec{q},\omega) = \frac{S^2}{4\pi^{5/2}} \frac{n_v}{\bar{u}} \frac{|f(q)|^2}{q} \exp\{-\frac{\omega^2}{(\bar{u}q)^2}\} \quad . \tag{4.6}$$

The c.p. width

$$\Gamma_z(q) = \bar{u}q \tag{4.7}$$

has a linear q-dependence that is very well supported by our MC-MD data.[40] The c.p. intensity is

$$I_z(q) = (2\pi)^{-2} n_v S^2 |f(q)|^2 \quad . \tag{4.8}$$

In order to calculate the form factor (4.4) we have taken[40] $\theta(r)$ from the continuum theory of Hikami and Tsuneto[21] for a static vortex. The asymptotic solution is

$$\theta(r) = \frac{\pi}{2}[1 \pm \exp(-r/r_v) \quad , \quad r \gg r_v \quad , \tag{4.9}$$

with

$$r_v = r_v^{HT} = a/\sqrt{2(1-\lambda)} \quad , \tag{4.10}$$

where λ is the anisotropy parameter in the Hamiltonian (1.1) and a is the lattice parameter. For $qr_v \ll 1$ the form factor (4.4) can be approximated analytically (Appendix A) by

$$f(q) \simeq \frac{\pi_v^2 r^2}{[1 + (qr_v)^2]^{3/2}} \quad , \quad qr_v \ll 1 \quad . \tag{4.11}$$

For small q the resulting intensity $I_z(q)$ is qualitatively consistent with our MC-MD data for the XY model, but the absolute intensity differs by one order of magnitude.[40]

However, in the meantime it has been noted[41] that the theory of Hikami and Tsuneto[21] is incomplete because a certain term is missing in their Hamiltonian; consequently the same holds for the Euler-Lagrange equation for $\theta(r)$.

The correct equation for $\theta(r)$ is identical with the static limit of the Landau-Liftshitz equation $d\vec{S}_n/dt = \{\vec{S}_n, H\}$ in the continuum limit.[41,42] The asymptotic solution is formally the same as (4.9), but the vortex-core radius now is

$$r_v = \frac{a}{2}\left(\frac{\lambda}{1-\lambda}\right)^{1/2} \quad . \tag{4.12}$$

This difference, compared to (4.10), turns out to be decisive because for $\lambda = 0$ we get $r_v = 0$ and thus $f(q) \equiv 0$. (This result has been checked by a MD-simulation starting with a single vortex at rest;[41] in fact for $\lambda = 0$, and also for $\lambda \ll 0.8$, no out-of-plane structure is found, in contrast to $0.8 \leq \lambda < 1$.)

The result $f(q) \equiv 0$ means that $S_{zz}(\vec{q},\omega)$ would also vanish which is in clear contradiction to our observation of a central peak in the MC-MD simulations for the XY model.[40] Therefore, we now conclude that the static approximation for the out-of-plane structure of moving vortices is not valid for $\lambda \ll 0.8$, for $0.8 \leq \lambda < 1$ it may be used as a first approximation.

It will be necessary to solve the equations of motion for a single vortex, which exceeds the frame of this paper. Our theory for

the in-plane correlations in not affected at all because we have only used the fact that a moving vortex changes as $\theta(\vec{r},t)$ by a factor of (-1). However, the out-of-plane correlations are directly influenced by the velocity dependence of $\theta(\vec{r})$ and $f(\vec{q})$. Instead of (4.5), now

$$S_{zz}(\vec{q},t) = \left(\frac{S}{2\pi}\right)^2 n_v \int^2 d\,u\, |\vec{f}(\vec{q},u)|^2 \; \vec{P}(u)\bar{e}^{i\vec{q}\vec{u}t} \qquad (4.13)$$

must be calculated. For $S_{zz}(\vec{q},\omega)$ we expect again a Gaussian central peak. However, the intensity $I_z(\vec{q}) = S_{zz}(\vec{q},t=0)$ will be quite different from (4.8) and (4.11). Moreover it will be necessary to improve the MC-MD data for the intensity. So far our data still scatter because it is difficult to subtract the softened spin-wave peak which appears together with the central peak[40] (for the in-plane correlations this problem occurs only for large q, see section 2).

Finally alternative c.p. mechanisms must be investigated which may also produce central components in $S_{zz}(\vec{q},\omega)$: vortex-magnon interactions and multi-magnon difference processes (c.f. the 1-d case[28]), as well as diffusive processes, which certainly become dominant for $T \gg T_c$ in the hydrodynamic regime[15] $q \lesssim n_v^{1/2}$.

5. Conclusion

Our vortex-gas phenomenology predicts a Gaussian central peak for the out-of-plane correlations, and a squared Lorentzian central peak for the in-plane ones (in addition to the spin-wave peaks). The central peaks are produced by quite different mechanisms, depending on whether the correlations are locally or globally sensitive to the presence of vortices.

For the in-plane correlations the q-dependencies of the width and intensity of the central peak are in good agreement with the results from our MC-MD simulations. There are two parameters in the phenomenology that can be fitted: the correlation length ξ (half the average distance between the vortices), and the r.m.s. velocity $\bar{u}$. We obtain values for the parameters that agree rather well with the KT-theory[1,22] for ξ, and Huber's theory[15] for $\bar{u}$, which uses an equation of motion for the vortices.

For the in-plane form factor, Lorentzian central peaks have been measured by inelastic neutron scattering for two materials. From the theory we obtain qualitatively the same wave vector and temperature dependencies, but a smaller width. Of course, extrinsic damping and pinning mechanisms will result in slower vortex timescales than our estimates.

So far the experimental data have been fitted to an ad hoc formula, namely to a product of a Lorentzian for the ω-dependence and another Lorentzian for the q-dependence. A fit to our squared Lorentzian with its q-dependent width may allow a detailed comparison between theory and experiment and a measurement of the parameters $\bar{u}$ and ξ. However, depending on the particular material, the present theory has to be modified in order to take into account different lattice structures, competing interactions, and in-plane anisotropies. Similarly to the 1-D case,[37,38] we expect that quantum effects will primarily[39] lead to renormalizations of the parameters, but fundamental questions of quantum dynamics remain here as in 1-D spin systems. For the out-of-plane correlations the dynamic form factor has proven difficult to measure. Our MC-MD simulations show a central peak. The width depends linearly on q, as predicted. However, the intensity has not yet been calculated

because the velocity dependence of the out-of-plane structure of vortices has yet to be calculated.

Finally, in order to explain the absolute intensity of the central peaks, alternative mechanisms, e.g. vortex-magnon interactions and multi-magnon difference processes, must be included, as was necessary for 1-D cases.[28]

Acknowledgments

We are grateful to M. T. Hutchings, W. C. Kerr and S. Trugman for valuable discussions and correspondence. The research of FGM was partially supported by the travel grants ME 534/2-1 and 534/3-1 from the German Science Foundation. Work at Los Alamos was supported by the USDOE.

Appendix A

In the form factor (4.4), the angular integration can be performed to give

$$f(q) = 2\pi \int_0^\infty dr\, J_0(qr)\cos\,\theta(r)r \quad , \tag{A1}$$

where J_0 is a Bessel function of the first kind. Extending the asymptotic solution (4.9) to small r,

$$\cos\,\theta\,(r) \sim \sin(\frac{\pi}{2}\, e^{-r/r_v}) \tag{A2}$$

is a good approximation, since (A2) approaches one for $r \to 0$, as required by the correct solution (2.3b). Moreover, any error is suppressed by the factor r in the integrand in (A1).

In order to obtain approximate analytical results, we expand (A2) to first order in $\frac{\pi}{2}\exp(-r/r_v)$, which is small for $r >> r_v$. This gives eventually (4.11), valid for $qr_v << 1$.

Appendix B

We assume that all vortices have the same velocity $u = |\vec{u}|$, and average over u later. We want to show that the arguments used for the calculation of (2.4) in the 1-D case also hold in higher dimensions.

Let an "event" be the passing of a vortex through a contour connecting $(\vec{0},0)$ and $(\vec{r},t)$. We choose a contour consisting only of horizontal or vertical lines in the space-time diagram. Events at the same point $\vec{r}$ at different times (i.e. on a vertical line) are correlated if $t \leq r/u$, i.e. if the vertical line is outside the light cone $r = ut$. On the other hand, events at the same time t but at different points $\vec{r}$ (horizontal lines) are correlated if $r \leq ut$ (i.e. if events occur inside the light cone). Correlated events lead to a cancellation of factors (-1) in (2.4). The cancellation is complete for an even number of events, which is the case if we assume an isotropic velocity distribution.

There are now two cases. For $r \geq ut > 0$, we choose the contour $(\vec{0},0) \rightarrow (\vec{r},0) \rightarrow (\vec{r},t)$. The second part is a vertical line outside the light cone and therefore does not contribute. For the first part the events are not correlated, and we can directly calculate

$$\langle(-1)^{N(\vec{r},t)}\rangle = \sum_n (-1)^n p(n) = e^{-2\bar{n}} = e^{-r/\xi} \quad . \tag{B1}$$

Here n is the number of vortices passing between $\vec{0}$ and $\vec{r}$ at time t = 0, $\bar{n} = r/(2\xi)$ is their average number, and p(n) is the Poisson distribution. Similarly, in the second case ($ut \geq r > 0$) only the first part of the contour $(\vec{0},0) \rightarrow (\vec{0},t) \rightarrow (\vec{r},t)$ contributes and gives

$$\langle(-1)^{N(\vec{r},t)}\rangle = \sum_m (-1)^m p(m) = e^{-2\bar{m}} = e^{-ut/\xi} \quad . \tag{B2}$$

Here m is the number of vortices passing $\vec{r} = 0$ within the time t and $\bar{m}$ the average number.

The cases (B1) and (B2) can be combined to give

$$\langle(-1)^{N(\vec{r},t)}\rangle = \exp\left\{-\frac{|r - ut|}{2\xi} - \frac{|r + ut|}{2\xi}\right\} \quad . \tag{B3}$$

Using a Maxwellian velocity distribution, we get in the 2-D case

$$\tilde{P}(u) = 2\,\frac{u}{\bar{u}^2}\,\exp\left[-(u/\bar{u})^2\right] \tag{B4}$$

for the distribution of the moduli. A straightforward integration finally leads to (2.7).

Appendix C

Performing the temporal Fourier transform of (2.8) first gives

$$S_{xx}(\vec{r},\omega) = \frac{S^2}{2\pi}\frac{r}{\gamma\xi^2\alpha}K_1(\alpha r) \quad , \tag{C1}$$

with $\alpha = (\gamma^2 + \omega^2)^{\frac{1}{2}}/\gamma\xi$ and K_1 a modified Bessel function. For the 2-D spatial transform we use polar coordinates and find[31]

$$S_{xx}(\vec{q},\omega) = \frac{S^2}{(2\pi)^2}\frac{1}{\gamma\xi^2\alpha}\int_0^\infty dr\, r^2\, K_1(\alpha r)\, J_0(qr) \tag{C2}$$

$$= \frac{S^2}{2\pi^2\gamma\xi^2\alpha^4}F(2,1;1;-q^2/\alpha^2) \quad , \tag{C3}$$

where J_0 is a Bessel function of the first kind, and F a hypergeometric function which reduces[31] in this case to $(1 + q^2/\alpha^2)^{-2}$, leading eventually to the result (2.9).

Appendix D

The numerical calculations were performed on a CRAY-1 machine. This enabled the use of a vectorized MC algorithm, by updating spins on the even and odd sublattices separately. Periodic boundary conditions were applied for both the MC and MD simulations.

The timestep used in the Runge-Kutta integration was 0.04, and 512 samples of the spin configuration were saved at time intervals of NS × 0.04, with NS = 8, 16 or 32, depending on the frequency range of interest. The space-time Fourier-transformed data was then smoothed to reduce the noise due to statistical fluctuations, by convolution of a five-point smoothing function $f(\omega)$ with $S(\vec{q},\omega)$. (Five points on the frequency grid were used.) The function f was taken as a discrete approximation to a parabola.

$$f(\omega) \propto 1 - (\omega/w)^2 \quad , \quad w = (7/3)\,\Delta\omega \quad ,$$

where $\Delta\omega$ was the ω-grid spacing, $2\pi/T$, with T the total time of integration. This makes the relative weights of the five points in the convolution averaging procedure 0.27, 0.82, 1.0, 0.82 and 0.27.

Appendix E

The spin-wave contribution to the in-plane static correlation function is $\sim r^{-\eta}$, where $\eta(T)$ is a critical exponent.[22] Performing the angular integrations in the Fourier transformation the intensity of the spin-wave peak is

$$I_x^{sw}(q) \sim \int_0^\infty dr\, r^{1-\eta}\, J_0(qr) \quad , \tag{E1}$$

where J_0 is a Bessel function of the first kind. In order to ensure a finite result a cutoff is necessary. We choose to introduce a factor $\exp(-\varepsilon r)$ into the integrand, with $\varepsilon = O(L^{-1})$, where L is the (linear) size of the lattice. Then the integration yields[31]

$$I_x^{sw}(q) \sim \frac{F(1-\eta/2,-1/2+\eta/2;\ 1;\ q^2/(\varepsilon^2+q^2))}{(\varepsilon^2+q^2)^{1-\eta/2}} \tag{E2}$$

where F is a hypergeometric function.

For $T < T_c$ this can be compared directly with the total intensity $I_x^{tot} = S_{xx}(q,t=0)$ from our MC simulations. For $q = O(L^{-1})$ we indeed see a size dependence that is qualitatively similar to that of (E2). For $q \gg L^{-1}$ the form (E2) reduces to $I_x^{sw} \sim q^{-(2-\eta)}$; this q-dependence is reproduced very clearly by our MC data.

The case $T > T_c$ is discussed in section 2.

References

1. J. M. Kosterlitz and D. J. Thouless, J. Phys. C 6, 1181 (1973); Prog. Low Temp. Phys. Vol VIIB, Chapt. 5, ed. D. F. Brewer (North-Holland, Amsterdam, 1978).

2. K. Hirakawa, H. Yoshizawa, and K. Ubukoshi, J. Phys. Soc. Japan 51, 2151 (1982); K. Hirakawa, H. Yoshizawa, J. D. Axe, and G. Shirane, NEW. TOP. Satellite Conf. of ICM'82 (1982).

3. M. T. Hutchings, J. Als-Nielson, P. A. Lindgard and P. J. Walker, J. Phys. C14, 5327 (1981).

4. L. P. Regnault, J. Rossat-Mignod, and J. Y. Henry, J. Phys. Soc. Japan 52, suppl. 1 (1983); L. P. Regnault, J. Rossat-Mignod, J. Y. Henry, R. Pynn and D. Petitgrand, in "Magnetic Excitations and Fluctuations," eds. S. W. Lovesey, N. Balucani, F. Borsa, and V. Tognetti, Springer Series in Solid State Sciences Vol. 54, p. 201, (Springer, Berlin, 1984).

5. L. P. Regnault and J. Rossat-Mignod, in "Magnetic Properties of Layered Transition Metal Compounds," eds. L. J. de Jongh and R. D. Willet (Reidel, Dordricht, 1987).

6. M. Elahy and G. Dresselhaus, Phys. Rev. B 30, 7225 (1984).

7. See articles in "Magnetic Properties of Low-Dimensional Systems," eds. L. M. Falicov and J. L. Moran-Lopez (Springer-Verlag 1986).

8. H. J. Mikeska, J. Phys. C 11, L29 (1978); J. Phys. C 13, 2313 (1980).

9. M. Steiner and A. R. Bishop, in "Solitons", eds. V. L. Pokrovskii, S. E. Trullinger, and V. E. Zakharov (North-Holland, Amsterdam, 1986).

10. D. J. Bishop and J. D. Reppy, Phys. Rev. Lett. 40, 1727 (1978); V. Ambegaokar, B. I. Halperin, D. R. Nelson and E. G. Siggia, Phys. Rev. B 21, 1806 (1980).

11. A. F. Hebard and A. Fiory, Phys. Rev. Lett. 44, 291 (1980); B. I. Halperin and D. R. Nelson, J. Low Temp. Phys. 36, 599 (1979).

12. S. R. Shenoy, J. Phys. C 18, 5163 (1985).

13. D. R. Nelson and D. S. Fisher, Phys. Rev. B 16, 4945 (1977).

14. R. Côté and A. Griffin, Phys. Rev. B 34, 6240 (1986).

15. D. L. Huber, Phys. Lett. 76A, 406 (1980), Phys. Rev. B26, 3758 (1982).

16. C. Kawabata, M. Takeuchi, A. R. Bishop, J. Magn. Magn. Mat. 54-57, 871 (1986), J. Stat. Phys. 43, 869 (1986).

17. M. T. Hutchings, P. Day, E. Janke, and R. Pynn, J. Magn. Magn. Mat. 54-57, 673 (1986).

18. L. P. Regnault, J. P. Boucher, J. Rossat-Mignod, J. Bouillot, R. Pynn, J. Y. Henry, and J. P. Renard, Physica 136B, 329 (1986).

19. C. Kawabata and A. R. Bishop, Sol. State Comm. 42, 595 (1982), J. Phys. Soc. Japan 52, 27 (1983).

20. C. Kawabata and A. R. Bishop, Sol. State Comm. 60, 169 (1986).

21. S. Hikami and T. Tsuneto, Progr. Theor. Phys. 63, 387 (1980).

22. J. M. Kosterlitz, J. Phys. C7, 1046 (1974).

23. J. Villain, J. de Phys. 35, 27 (1974); 36, 581 (1975).

24. J. V. José, L. P. Kadanoff, S. Kirkpatrick, and D. R. Nelson, Phys. Rev. B 16, 1217 (1977).

25. S. W. Heinekamp and R. A. Pelcovitz, Phys. Rev. B 32, 4528 (1985); R. A. Pelcovitz, Phys. Rev. A 14, 1693 (1981).

26. J. Tobochnik and G. V. Chester, Phys. Rev. B 20, 3761 (1979), R. Loft and T. A. DeGrand, preprint.

27. D. R. Nelson and J. M. Kosterlitz, Phys. Rev. Lett. 39, 1201 (1979).

28. E. Allroth and H. J. Mikeska, J. Phys. C 13, L 725 (1980), Z. Physik B 43, 209 (1981).

29. S. N. Dorogovtsev, Sov. Phys. Sol. State 21, 43 (1979).

30. H. Takayama and K. Maki, Phys. Rev. B 21, 4558 (1980).

31. I. S. Gradshteyn and I. M. Ryzhik, Table of Integrals, Series, and Products (Academic Press, New York, 1980).

32. D. L. Huber, Phys. Lett. 68A, 125 (1978).

33. C. Kawabata and A. R. Bishop, Sol. State Comm. 33, 453 (1980).

34. A. A. Belavin and A. M. Polyakov, JETP Lett. 22, 503 (1975).

35. cf. MC-Simulations by S. Tang and S. D. Mahanti, Phys. Rev. B33, 3419 (1986); however, they consider a different anisotropy from that in $BaCo_2(AsO_4)_2$.

36. C. A. Cornelius, P. Day, P. J. Fyne, M. T. Hutchings and P. J. Walker, J. Phys. C 19, 909 (1986).

37. E. Loh Jr., D. J. Scalapino, and P. M. Grant, Phys. Rev. B 31, 4712 (1985).

38. G. M. Wysin and A. R. Bishop, Phys. Rev. B 34, 3377 (1986).

39. For spin-1/2, alternative descriptions of the ordering and phase transition have been proposed (e.g. D. D. Betts and S. B. Kelland, J. Phys. Jpn. 52, Suppl. p. 11 (1983)) in which vortices are not the dominant excitations.

40. F. G. Mertens, A. R. Bishop, G. M. Wysin and C. Kawabata, Phys. Rev. Lett. 59, 117 (1987).

41. M. E. deGouvea, A. R. Bishop, G. M. Wysin, F. G. Mertens, to be published.

42. S. Takeno and S. Homma, Progr. Theor. Phys. 64, 1193 (1980).

Table 1. Parameters $\bar{u}$ and ξ obtained by fitting to the widths and intensities of the central peaks in our MC-MD data for the XY model ($\lambda = 0$), compared to independent theoretical predictions in the last column (using $T_c = 0.8$, $\xi_0 = a$, and estimating b from Fig. 9 of ref. 25).

		$\bar{u}$ from	
T	$\tau=T/T_c-1$	$\Gamma_x(q)$	Eq. (2.13)
0.9	0.125	0.84	0.30(b=0.5)
1.0	0.25	0.91	0.47(b=0.4)
1.1	0.375	0.91	0.56(b=0.3)

		ξ/a from		
T	$\tau=T/T_c-1$	$\Gamma_x(q)$	$I_x(q)$	Eq. (1.3)
0.9	0.125	4.8	4.4	4.1(b=0.5)
1.0	0.25	3.0	2.4	2.2(b=0.4)
1.1	0.375	1.9	2.1	1.6(b=0.3)

Figure Captions

Fig. 1. (a) A vortex passes the origin at time t, the arrows indicate the spins $\vec{S}$. (b) the field $S_x = S \cos \phi$ is changed by a factor of (-1), independent of the direction of the motion.

Fig. 2 Dynamic structure factor for <u>in-plane</u> correlations from MC-MD, $\vec{q}$ in units of $2\pi/L$, with lattice size $L = 100$ a. Temperature $T = 0.5$ (- - -) and 1.1 (——), with $T_c \simeq 0.8$. (The data are smoothed according to Appendix D).

Fig. 3(a,b,c). Width Γ_x of central peak in $S_{xx}(\vec{q},\omega)$ for different temperatures T. Data points and error bars result from estimating Γ_x from plots like Fig. 5. Solid lines are fits to the width (3.8) of the squared Lorentzian (3.7).

Fig. 4(a,b,c) Intensity I_x of central peak in $S_{xx}(\vec{q},\omega)$ for different temperatures T. Data points result from estimating I_x from plots like Fig. 5, assuming a squared Lorentzian form. Solid lines are fits to (3.9) for small q.

Fig. 5. Spin-wave dispersion from MC-MD simulation of the anisotropic Heisenberg model (1.1) for two temperatures (above and below T_c). Lattice size $L = 100$ a. Solid lines are guides to the eye.

Fig. 6. Width Γ_x of central peak in $S_{xx}(\vec{q},\omega)$ for the anisotripic Heisenberg model ($\lambda = 0.8$). Data points and error bars result from estimating the width from plots like Fig. 2. Solid line is a fit for small q to (2.10).

(a)

$(S_x(\vec{r},t), S_y(\vec{r},t))$

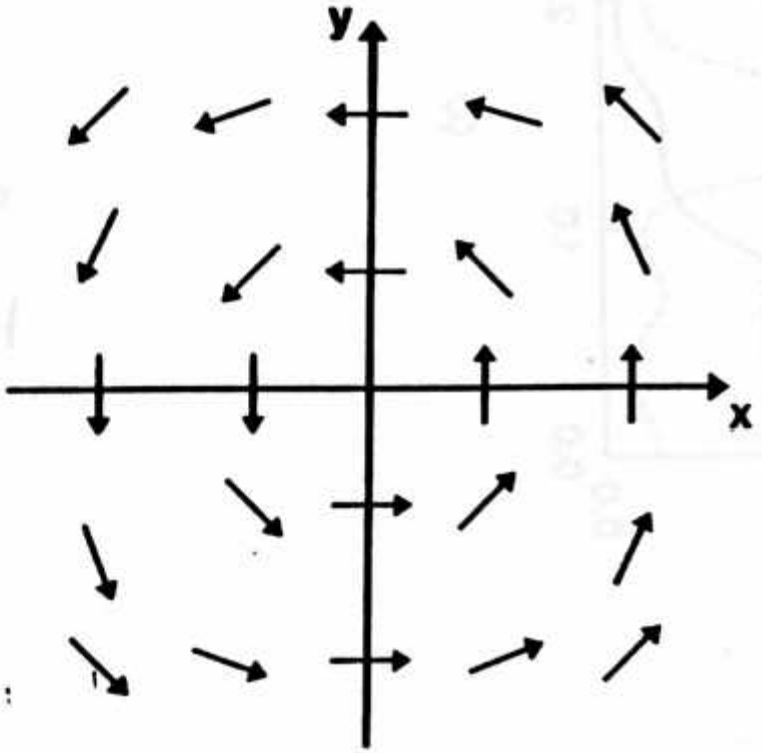

(b)

$\cos \phi(\vec{r},t)$

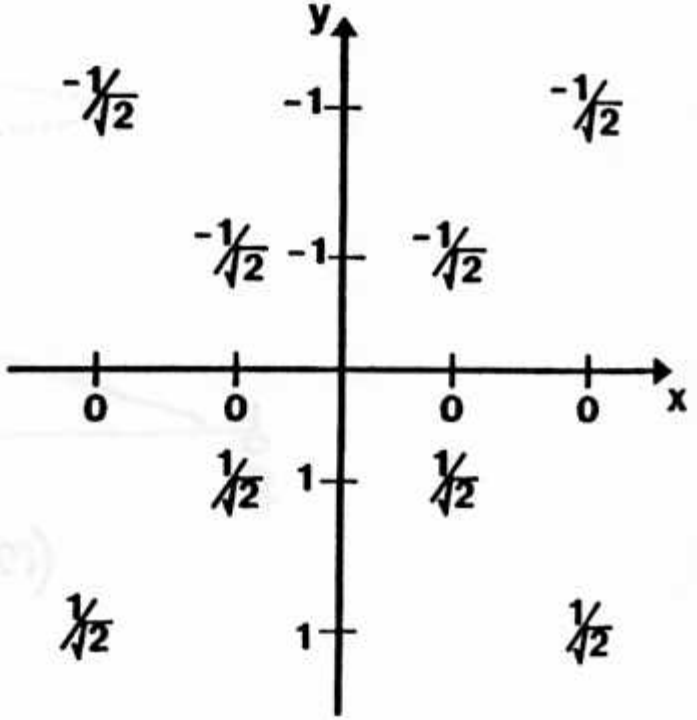

Los Alamos

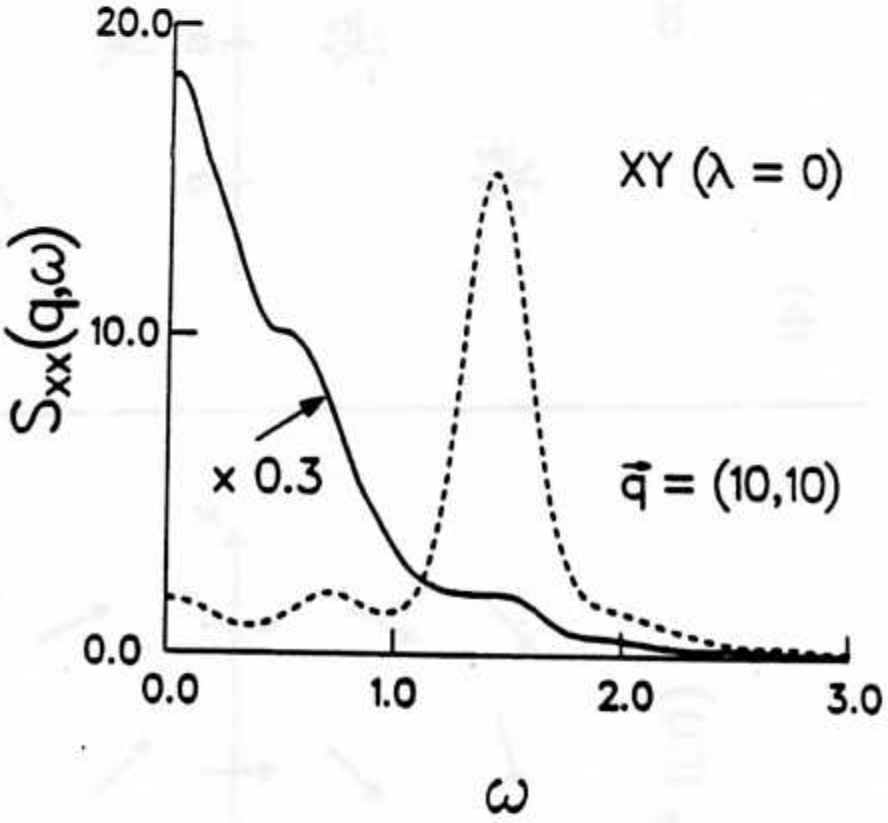
20.0
10.0
0.0
$S_{xx}(q,\omega)$
XY ($\lambda = 0$)
x 0.3
$\vec{q} = (10,10)$
0.0
1.0
2.0
3.0
ω

Fig. 2

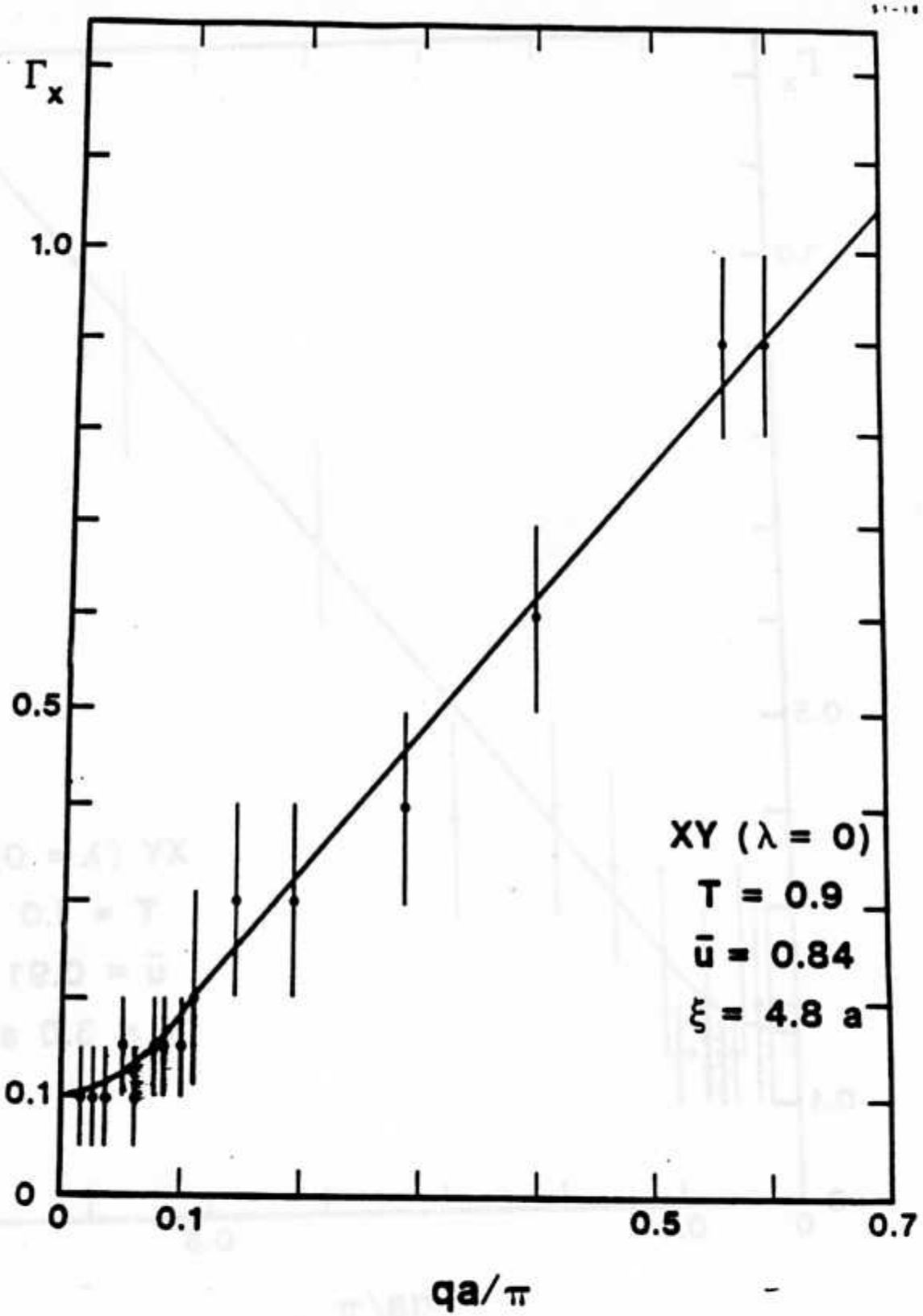

Los Alamos

Fig. 3 (a)

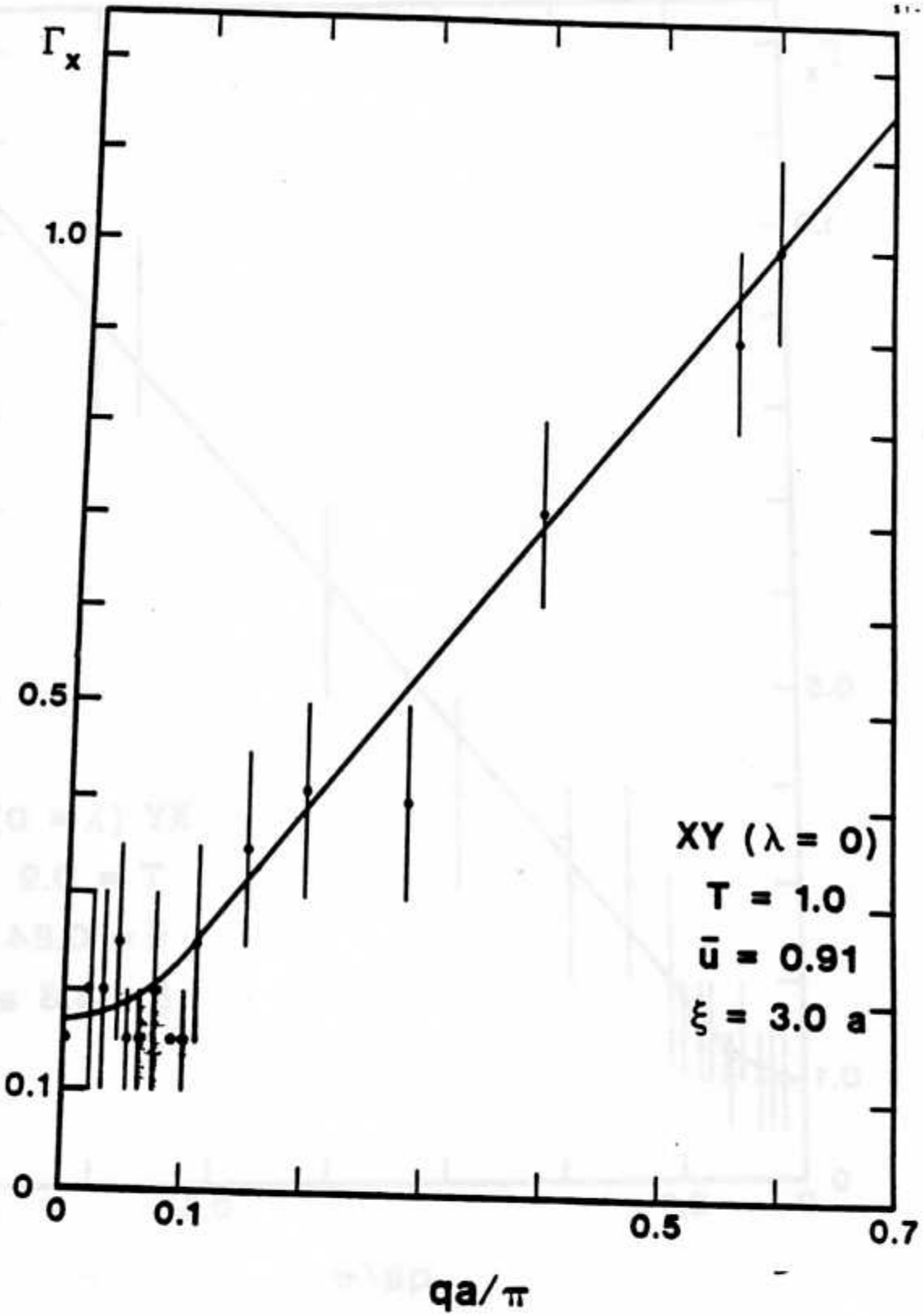

Los Alamos

Fig. 3 (b)

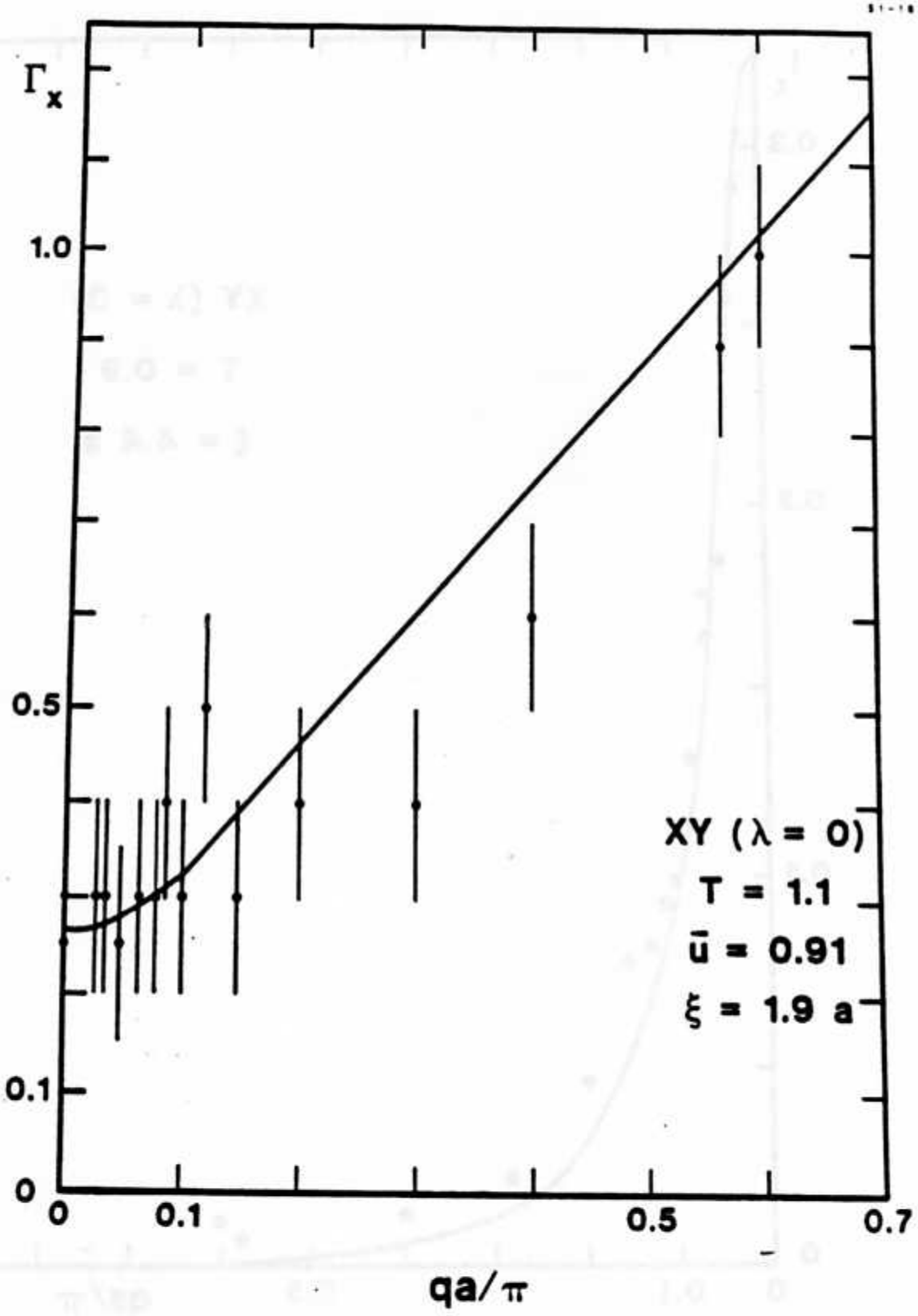

Los Alamos

Fig. 3 (c)

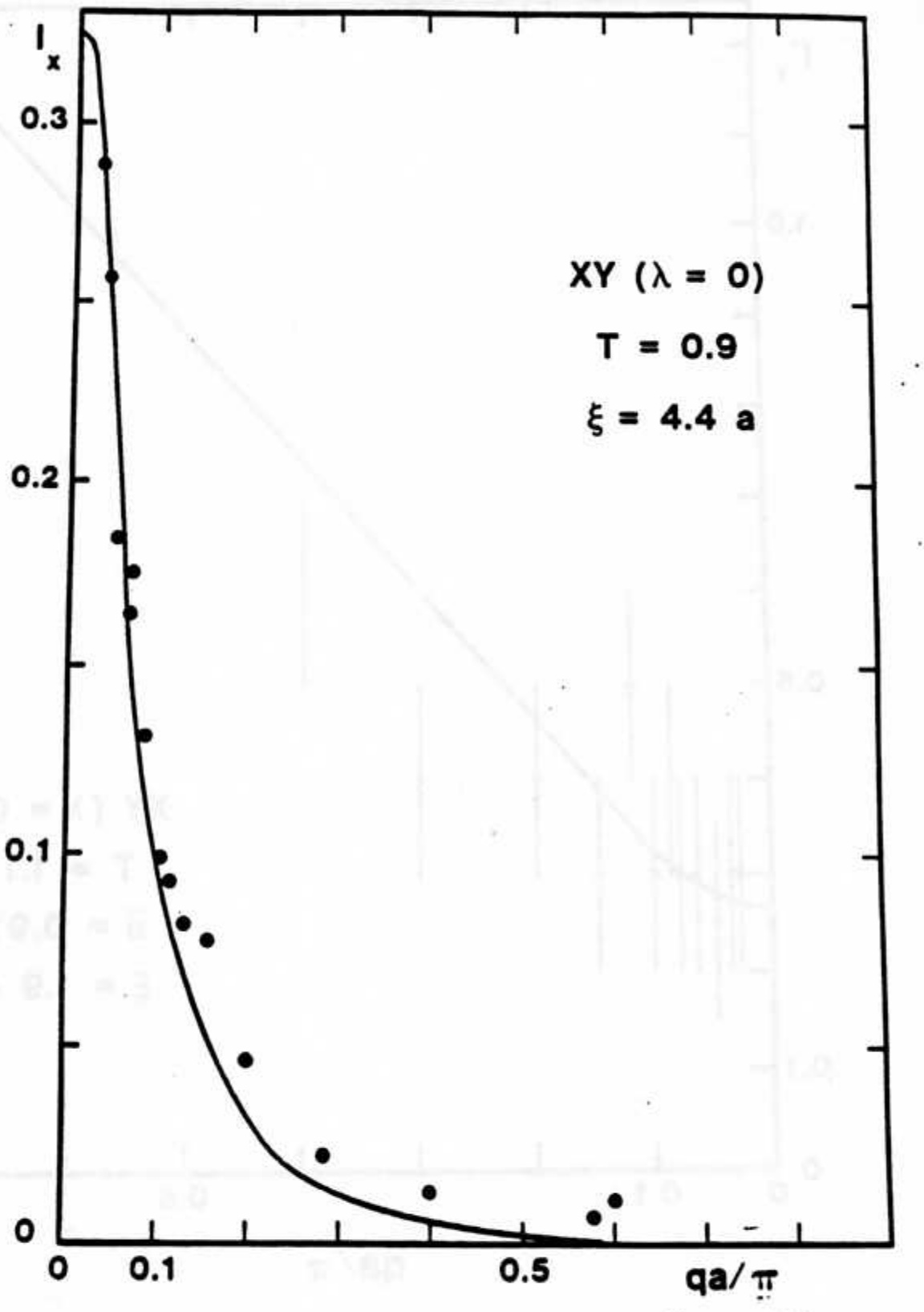

Fig. 4 (a)

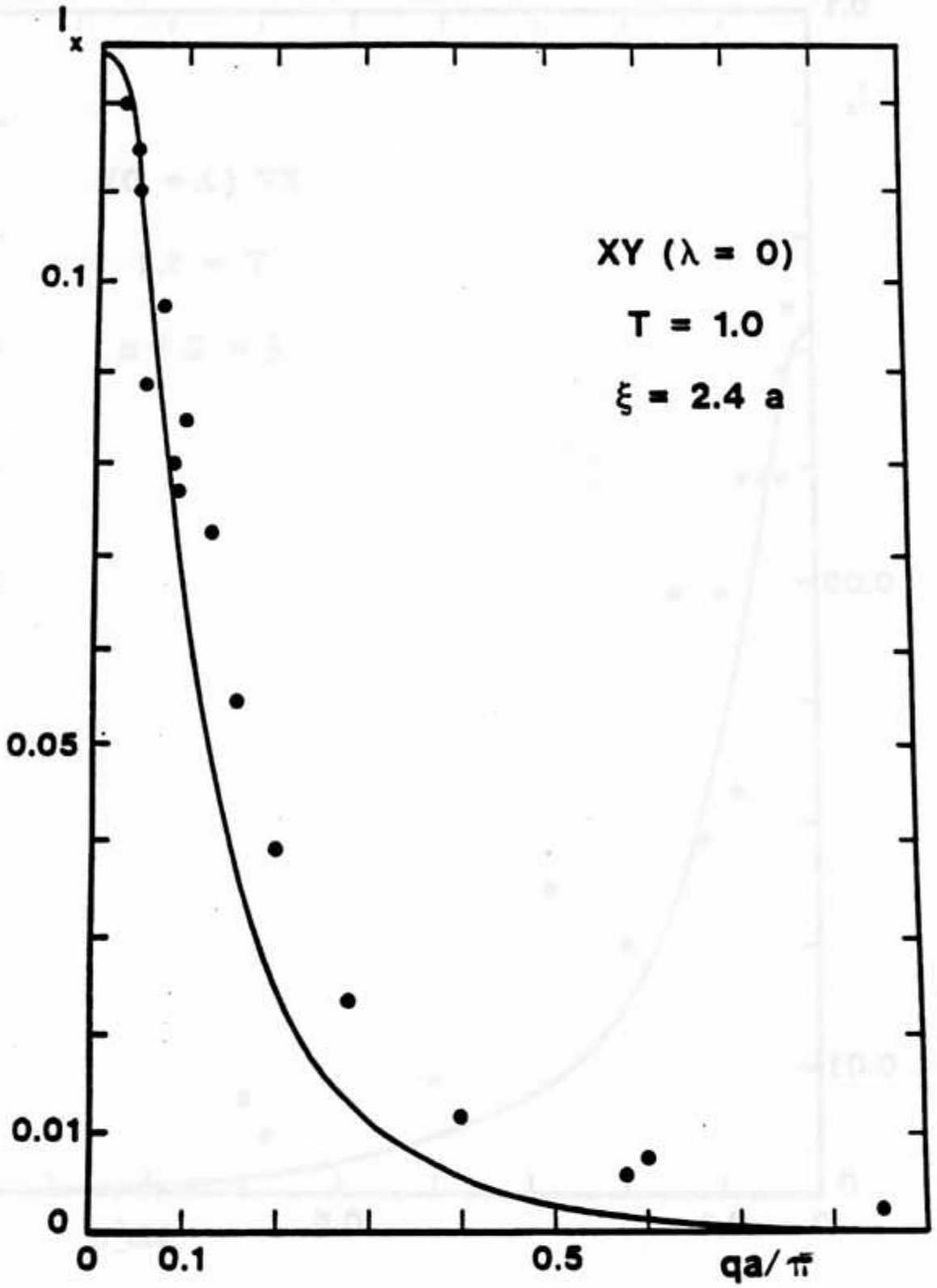

Los Alamos

Fig. 4(b)

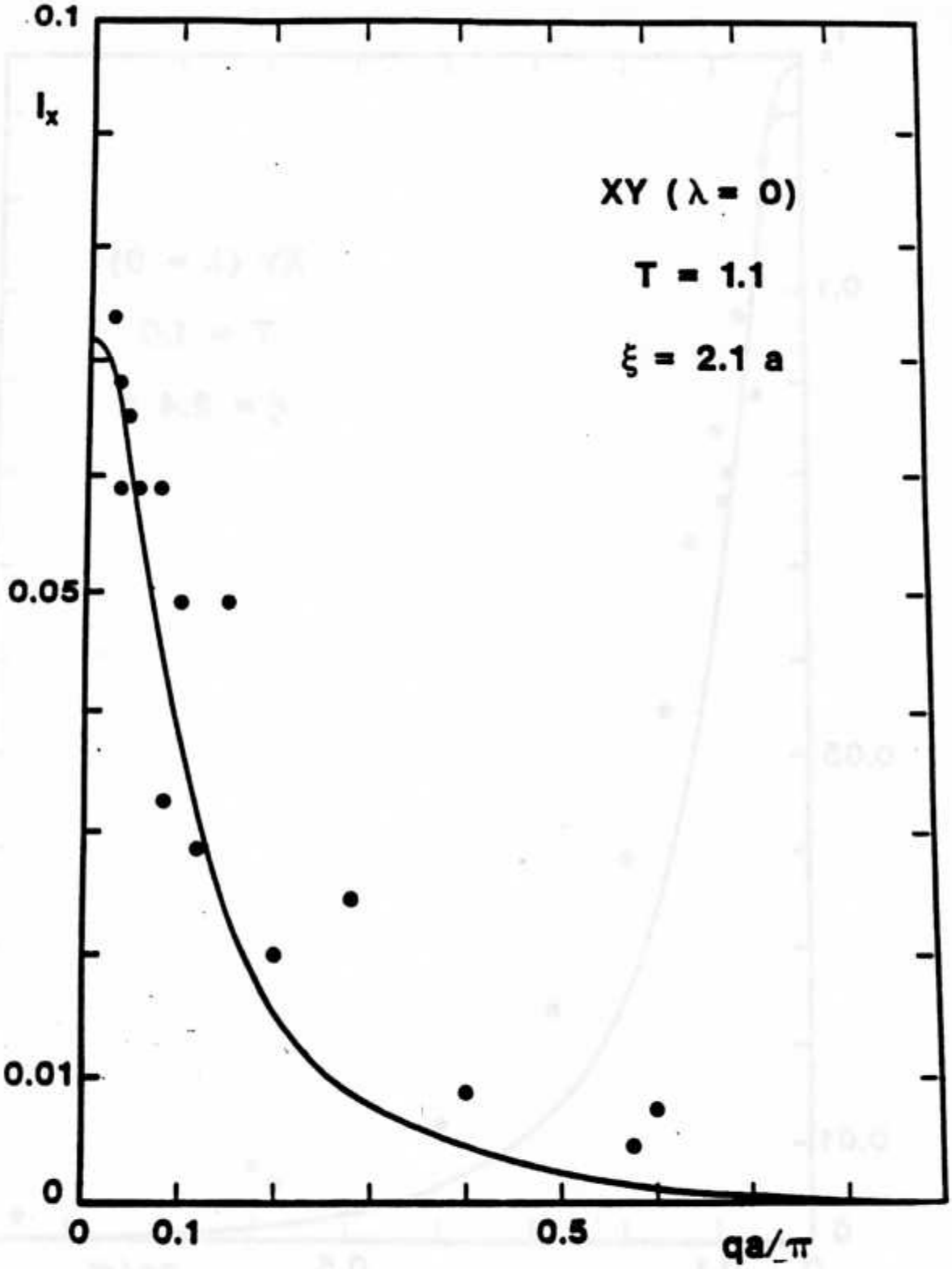

Los Alamos

Fig. 4 (c)

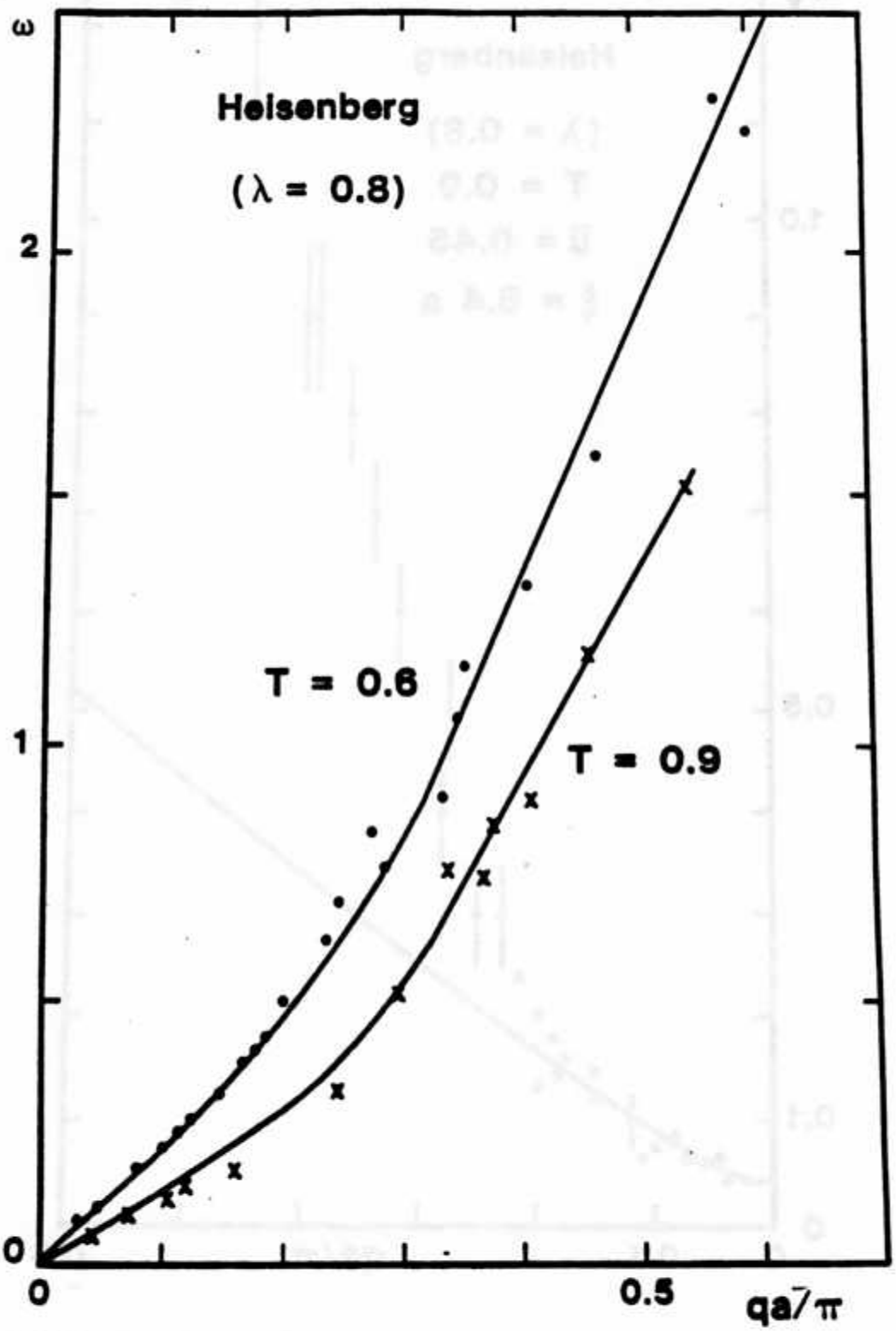

Los Alamos

Fig. 5

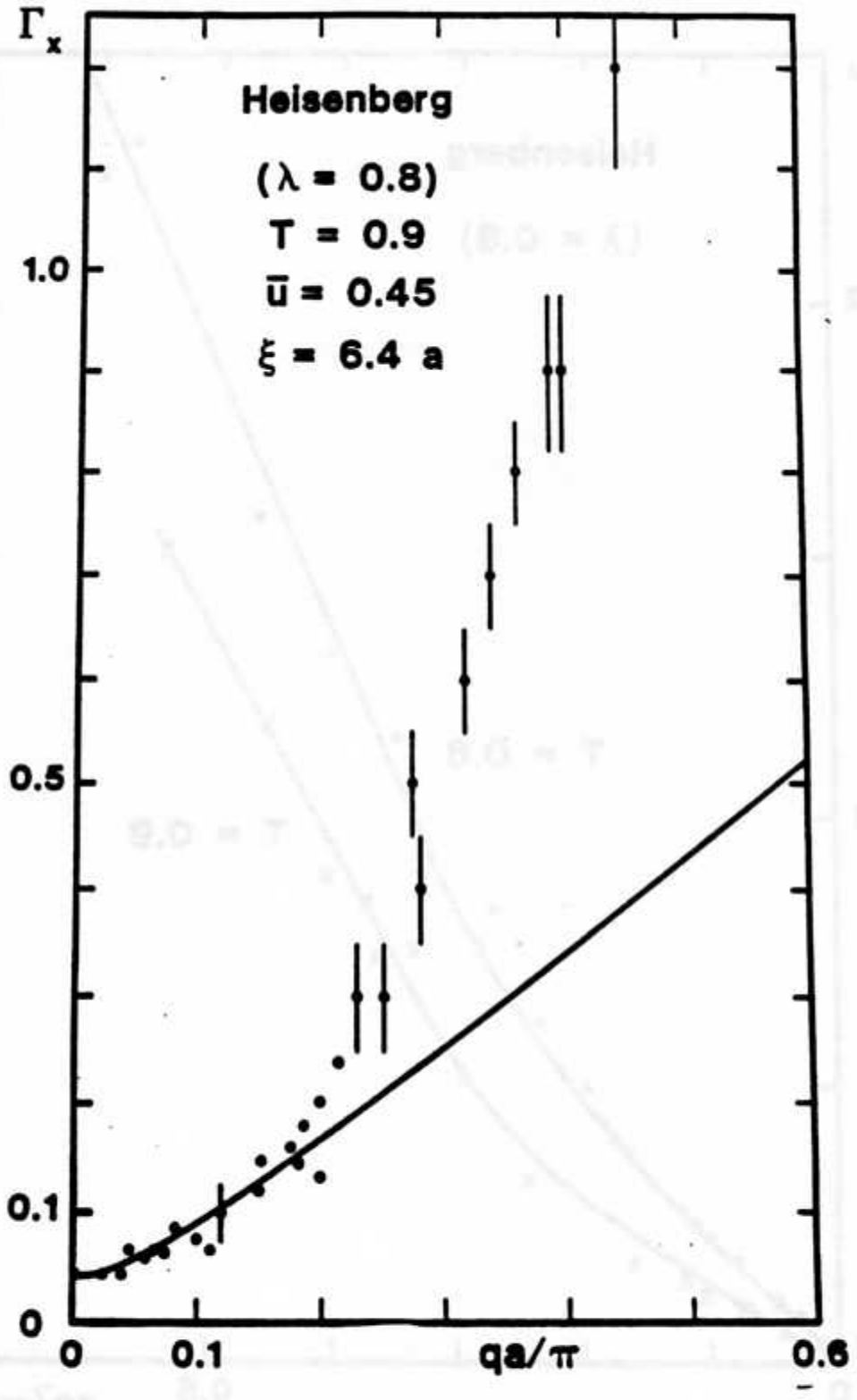

Los Alamos

Fig. 6